Carbohydrate Polymers 85 (2011) 37–43

Contents lists available at ScienceDirect

Carbohydrate Polymers

journal homepage: www.elsevier.com/locate/carbpol

Mannosylated chitosan-zinc sulphide nanocrystals as fluorescent bioprobes for targeted cancer imaging

Aswathy Jayasree [1], Sajith Sasidharan [1], Manzoor Koyakutty, Shantikumar Nair, Deepthy Menon *

Amrita Centre for Nanosciences and Molecular Medicine, Amrita Institute of Medical Sciences and Research Centre, Amrita Vishwavidyapeetham University, Cochin-682 041, Kerala, India

ARTICLE INFO

Article history:
Received 3 November 2010
Received in revised form 18 January 2011
Accepted 20 January 2011
Available online 28 January 2011

Keywords:
Bioimaging
Chitosan
D-Mannose
Mannose receptor
Nanocrystals
Oral cancer
Zinc sulphide

ABSTRACT

A novel nanomaterial based on chitosan-zinc sulphide:Mn (ZnS:Mn) conjugated with mannose ligand has been developed for targeted cancer imaging. The nanobioconjugates, prepared through simple aqueous chemistry, possessed high colloidal stability and strong fluorescence emission at ~600 nm. Characterization using XRD, DLS, SEM, AFM and FTIR revealed that the bioconjugated particles are appropriately functionalized and stable, with average size ~150 nm. The presence of polysaccharide chitosan bestowed enhanced biocompatibility to the nanocrystals and provided suitable functionality for mannosylation. *In vitro* cytotoxicity studies on mouse fibroblast (L929) and oral epithelial carcinoma (KB) cells confirmed their cytocompatibility. Bioconjugation with mannose provided specificity and targeted cellular labelling characteristics as demonstrated using KB cells which over-express mannose receptors on their surface. Our investigations highlight the applicability of polysaccharide protected and mannosylated fluorescent ZnS nanoprobes for active targeting of cancer cells.

1. Introduction

Nanosized particles with embedded luminescent features are of immense importance in analytical chemistry and bioengineering due to their potential applications in medical diagnostics, multiplexed bioassays, drug screening, etc. (Doty, Fernig, & Levy, 2004). Semiconductor nanocrystals, also known as quantum dots (QDs), have unique size-tunable spectral properties, excellent photostability, etc. (Gao, Cui, Levenson, Chung, & Nie, 2004), which provide substantial improvements in the sensitivity of molecular imaging and quantitative cellular analysis (Bruchez, Moronne, Gin, Weiss, & Alivisatos, 1998; Chan & Nie, 1998). By appropriate bio-conjugation, such nanocrystals can replace the conventional organic fluorescent dyes in immunostaining and bioimaging of tissues and cancerous cells (Medintz, Uyeda, Goldman, & Mattoussi, 2005; Smith, Duan, Mohs, & Nie, 2008). Surface modification of these QDs using biocompatible polysaccharides offer several advantages such as (i) passivation of the surface defects of QDs, with enhanced fluorescence (Hezinger, Tessmar, & Goepferich, 2008; Nie, Tan, & Zhang, 2006); (ii) biocompatibility to the otherwise toxic core of the QDs (Xie et al., 2005; Yu, Chang, Drezek, & Colvin, 2006); (iii) provide functional groups for further bioconjugation with suitable ligands (Jain et al., 2008; Mathew et al., 2010; Warad, Thanachayanont, Tumcharern, & Dutta, 2007). The versatility of chitosan, a natural biopolymer, facilitates chemical modifications, graft reactions, ionic interactions, etc. and hence would be an appropriate candidate for this purpose (Jayakumar, Menon, Manzoor, Nair, & Tamura, 2010; Kumar, Muzzarelli, Muzzarelli, Sashiwa, & Domb, 2004). In the present work, we have utilized this natural polysaccharide to surface passivate as well as enable bioconjugation of ZnS:Mn nanocrystals with a carbohydrate, *viz*, mannose, to target the mannose receptors over-expressed on cancer cells.

The cytotoxicity arising from heavy-metal based QDs of CdS, CdSe, CdTe, CdSe/ZnS, etc. (Lovric, Sung, & Francoise, 2005; Mattoussi et al., 2001) necessitates the development of heavy-metal free materials that are predominantly biocompatible and aqueous based (Ashokan, Menon, Nair, & Manzoor, 2010; Pradhan, David, Liu, & Peng, 2007; Setua, Menon, Asok, Nair, & Manzoor, 2010). Recently, we have developed a heavy-metal free zinc sulphide based fluorescent nanocrystal for targeted cancer imaging using folic acid as the targeting ligand (Manzoor et al., 2009). We found that compared to many other known QDs, ZnS is a better system owing to its stable physical and chemical characteristics. Doped ZnS nanocrystals exhibit varying fluorescence depending upon the dopant selected, *viz*., Mn^{2+} yields an orange red emission

* Corresponding author. Tel.: +91 484 4008750; fax: +91 484 2802030.
E-mail addresses: deepthymenon@aims.amrita.edu, deepsmenon@gmail.com (D. Menon).
[1] These authors have contributed equally to the manuscript.

0144-8617/$ – see front matter © 2011 Elsevier Ltd. All rights reserved.
doi:10.1016/j.carbpol.2011.01.034

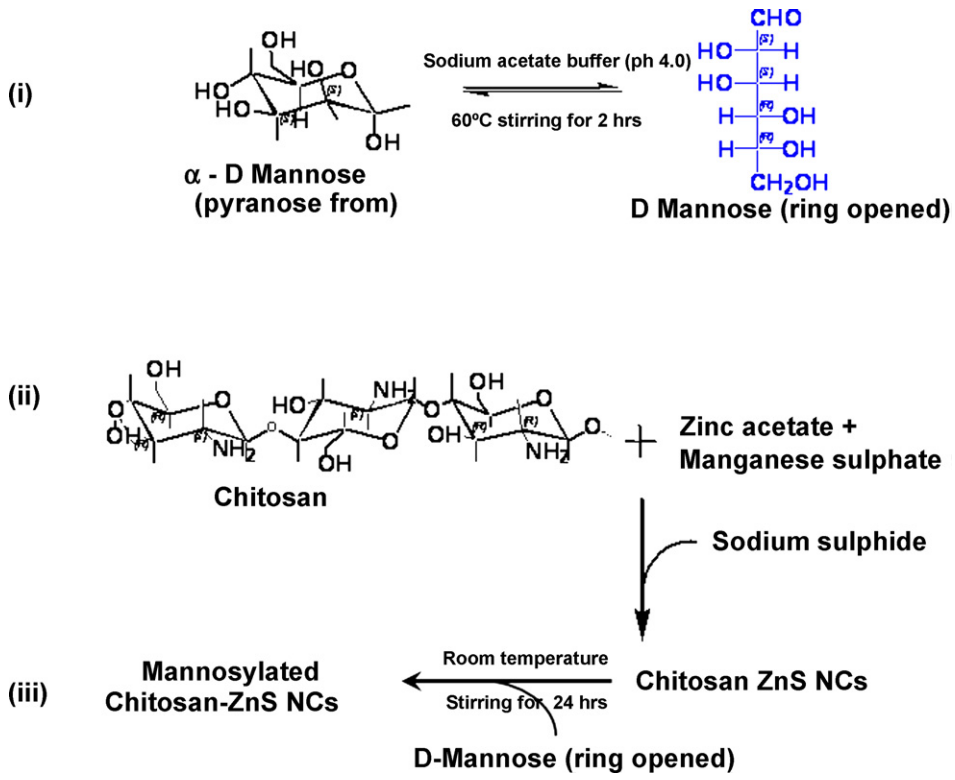

Fig. 1. Schematic representation of the synthesis scheme of mannosylated chitosan-ZnS NCs (i) ring opening of mannose sugar, (ii) *in situ* formation of chitosan-ZnS NCs and (iii) conjugation of chitosan-ZnS NCs with mannose.

(590 nm), Cu^{2+} a green emission (510 nm), etc. (Manzoor, Vadera, Kumar, & Kutty, 2003; Yang, Santra, & Holloway, 2005). Various polymers utilized for the surface passivation of ZnS (Lee et al., 2007; Li et al., 2004; Yang et al., 2005; Zhuang et al., 2003) were found to interact with the electronic transitions in the dopant ions and affect their fluorescence characteristics adversely. Hence, surface passivating agents that help to retain the important properties of the core material and also provide additional capabilities for bio-conjugation need to be probed. Thus, we have utilized here the well established chelation capacity of the amine groups of chitosan with transition metals such as Cu, Zn, Ni, Cd, etc. (Muzarelli, 2011) to couple the polysaccharide chitosan with ZnS through its surface zinc atoms. This also aids further functionalization with the targeting ligand D-mannose, enabling fluorescent detection of cancer cells. The over-expression of mannose receptors on a variety of tumors, macrophages, etc. has been taken to advantage in photodynamic therapy (Brevet et al., 2009), for drug or vaccine delivery and labelling macrophages (Kang, Cho, & Yoo, 2009), and hepatocytes in liver (Kikkeri, Lepenies, & Adibekian, 2009), targeted delivery to antigen presenting cells (Raiber et al., 2010), etc. However, no studies report the use of mannosylated fluorescent nanocrystals for targeted cancer diagnosis. Here we describe the targeted labelling of oral epithelial cancer cells (KB) using mannosylated chitosan-ZnS nanocrystals prepared through a simple and convenient aqueous chemistry route.

2. Materials and methods

2.1. Materials

Zinc acetate, sodium sulphide, manganese sulphate, high molecular weight chitosan with a degree of de-acetylation of 80% and D-mannose were obtained from Sigma Aldrich, USA. All the materials were used without further purification.

2.2. Preparation of mannosylated chitosan ZnS nanocrystals

Mannosylated chitosan-ZnS nanocrystals (mannosylated chitosan-ZnS NCs) were prepared by a two-step process involving (i) *in situ* synthesis of chitosan-ZnS nanocrystals (chitosan-ZnS NCs) and (ii) mannosylation of the above prepared NCs.

Chitosan-ZnS NCs were prepared by thoroughly mixing 1 ml of chitosan solution with the aqueous mixture of 10 ml 0.1 M zinc acetate [$Zn(CH_3COO)_2$] and 1.5 ml of manganese sulphate ($MnSO_4$) which yielded ~15 atomic% of Mn^{2+} ions with respect to the concentration of Zn^{2+} ions. After incubation for 20 min at room temperature, drop-wise addition of 10 ml 0.1 M sodium sulphide (Na_2S) to this mixture under constant stirring at room temperature resulted in the precipitation of chitosan-ZnS NCs. The pH of the solution was measured to be ~6 for optimal doping of Mn into the ZnS lattice, which is very critical to the formation of highly fluorescent nanocrystals. Varying concentrations of chitosan (0.001, 0.005, 0.01, 0.025, 0.05 wt%) were tested to get nanocrystals with optimum luminescence and stability. The white colloidal precipitate of chitosan-ZnS NCs was centrifuged at 6000 rpm for 10 min to remove the by-products as well as excess precursors. Centrifugation was repeated three times with distilled water and the nanocrystals were re-suspended in water. Spectrofluorimetric and zeta potential analysis were used to optimize the chitosan concentration.

Mannosylation of chitosan-ZnS NCs was carried out by adopting the method described by Mitchell, Roberts, Langley, Koentgen, and Lambert (1998) with certain modifications. The coupling of mannose to the amine groups of chitosan was carried out in two steps as depicted in Fig. 1. For this coupling reaction, initially, D-mannose (10 μM) was dissolved in 0.1 M sodium acetate buffer at pH 4 and 60 °C for 2 h, resulting in the ring opening of mannose molecules. In the second step, this solution was mixed thoroughly with chitosan-ZnS NCs synthesized earlier and incubated for 24 h at

room temperature. The aldehyde group of the ring opened mannose reacts with the amino groups of chitosan, yielding mannosylated chitosan-ZnS NCs. The resultant solution mixture was centrifuged at 5000 rpm and washed thoroughly in distilled water. The mannosylated chitosan-ZnS NCs were further purified by dialyzing against double-distilled water in a dialysis tube (MWCO 12–14 kDa; Himedia, Mumbai, India) for 24 h to remove any un-reacted mannose, salts, and partially mannosylated nanocrystals.

2.3. Physico-chemical characterization of nanocrystals

The particle size and size distribution of the prepared nanocrystals were characterized by the dynamic laser light scattering (DLS) technique [Nicomp 380 ZLS, Particle Sizing Systems, CA, USA] at a scattering angle of 90°. The intensity-weighted mean value was recorded as the average of three measurements.

The surface morphology of mannosylated chitosan-ZnS NCs was analyzed by scanning electron microscopy (JEOL JSM-649OLA, Japan). The samples were dropped on aluminium stubs, dried and then sputter coated with platinum by the Auto Fine Platinum Coater (JEOL, JFC-1600, Japan) before imaging.

Atomic force microscopy (JSPM 5200, JEOL, Japan) was also employed to study the particle size distribution of nanocrystals. Diluted samples (1:100 in distilled water) were dropped on atomically smooth mica sheet for AFM analysis and the measurements were performed in tapping mode.

The conjugation of chitosan and mannose to ZnS nanocrystals was confirmed using FTIR [Spectrum RX1 FTIR Spectrometer, Perkin Elmer, MA, USA] by recording the absorbance of samples in the frequency range from 4000 to 400 cm^{-1} with a 4 cm^{-1} resolution. The powder samples were mixed with KBr and pelletized before recording the IR spectra.

Crystallinity of bare ZnS NCs and mannosylated chitosan-ZnS NCs was studied using X-ray powder diffractometer [X'Pert PRO, PANalytical, The Netherlands] fitted with Cu-Kα source [λ = 1.541 Å]. The spectrum was recorded in the range from 5° to 70° at a step size of 0.02° and phase identification was done using JCPDS database.

Fluorescence spectral analysis of bare ZnS NCs, chitosan-ZnS NCs and mannosylated chitosan-ZnS NCs was carried out using a spectrofluorometer [FluoroMax-4, HORIBA, JOBIN YVON, USA]. The samples dispersed in MilliQ water were placed in a quartz cuvette and the fluorescence excitation and emission spectra were recorded after placing appropriate filters to avoid second order diffraction peaks.

2.4. Cell culture and in vitro toxicological analysis

Oral epithelial carcinoma KB cells and mouse fibroblast L929 cells (obtained from National Centre for Cell Science, Pune, India) were routinely grown in minimal essential medium (MEM) with 10% heat-inactivated fetal bovine serum (both from GIBCO-BRL, MD, USA) and 100 IU penicillin/streptomycin (GIBCO-BRL) at 37 °C in a humidified 5% CO_2 atmosphere. The cells were seeded in T25 flasks (BD Falcon, USA) at 5×10^5 cells per flask in 5 ml growth medium specific for KB.

Cytotoxicity of mannosylated chitosan-ZnS NCs and bare ZnS NCs was evaluated using MTT viability assay. KB and L929 cells were seeded at a density of 10^4 cells/ml in 96-well tissue culture plates [BD Bio Science, CA, USA] and incubated for 24 h for cell attachment. The medium was then replaced with fresh medium containing different concentrations (0.1–100 μM) of bare ZnS and mannosylated chitosan-ZnS NCs for 48 h at 37 °C. 10% FBS containing media was used as negative control and 1% Triton X100 served as positive control. Triplicates were set up for each sample concentration, negative and positive control. Optical absorbance was recorded at 570 nm using a microplate reader [Biotek Power Wave XS, Winooski, USA].

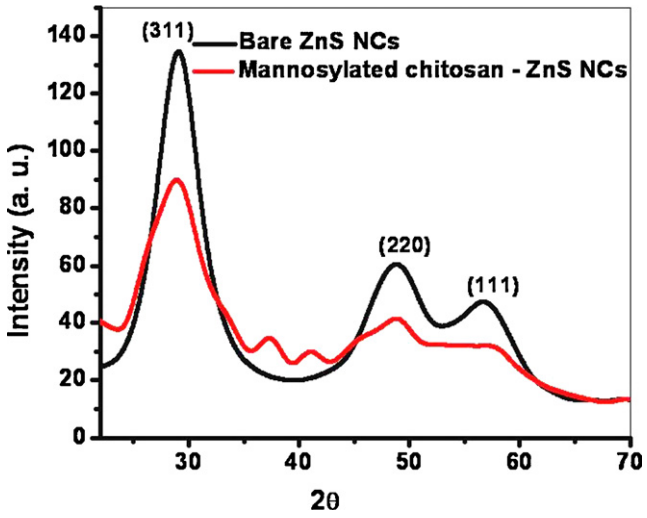

Fig. 2. X-ray diffraction patterns of bare ZnS NCs and mannosylated chitosan-ZnS NCs.

2.5. Fluorescence microscopy

Oral epithelial cancer, KB cells over express mannose receptors on their surface and hence were used as the test cells for fluorescence imaging studies (Agnani, Tricot-Doleux, Houalet, & Bonnaure-Mallet, 2003; Steele, Leigh, Swoboda, Ozenci, & Fidel, 2001). As negative control, we used the normal mouse fibroblast L929 cells grown in MEM medium, which do not have any expression of mannose receptors (Lane, Egan, Vick, Abdolrasulnia, & Shepherd, 1998). Cells (KB and L929) were seeded on 13 mm glass cover slips placed inside 24-well tissue culture plate at a seeding density of 3000 cells/cover slip. After 24 h, the adherent cells were washed once with PBS followed by replacement of media containing 150 μg/ml mannosylated chitosan-ZnS NCs and incubated for 1 h at 37 °C. Cells were washed once with PBS (300 μl/well), fixed with 2% paraformaldehyde for 20 min and mounted with DPX mounting medium. Imaging was done using Olympus BX-51 fluorescent microscope equipped with a CCD camera (Model DP71). Fluorescence was detected using band-pass excitation filter (330–385 nm) and high pass emission filter (420 nm) and 400 nm dichromatic mirror.

3. Results and discussion

3.1. Structural and optical characterization of mannosylated chitosan-ZnS NCs

Fig. 2 represents the X-ray diffraction pattern of bare ZnS NCs and mannosylated chitosan-ZnS NCs. Bare ZnS nanocrystals showed distinct peaks such as (1 1 1), (2 2 0) and (3 1 1) reflections at 28.63°, 48.055° and 57.45° respectively, correlating with the cubic zinc blend phase of ZnS. The XRD pattern of mannosylated nanocrystals showed broadened peaks of highly reduced intensities at 2θ values similar to those of ZnS, owing to the mannosylation of the polymer encapsulated ZnS NCs.

Fig. 3A and B represents the DLS spectra of chitosan-ZnS nanocrystals and mannosylated chitosan-ZnS nanocrystals respectively. The hydrodynamic diameter of chitosan-ZnS NCs was measured to be 90 ± 10 nm at optimal concentrations of chitosan (0.01 wt%). However, the average particle size measured using DLS was found to be increased to 150 ± 60 nm upon mannosylation

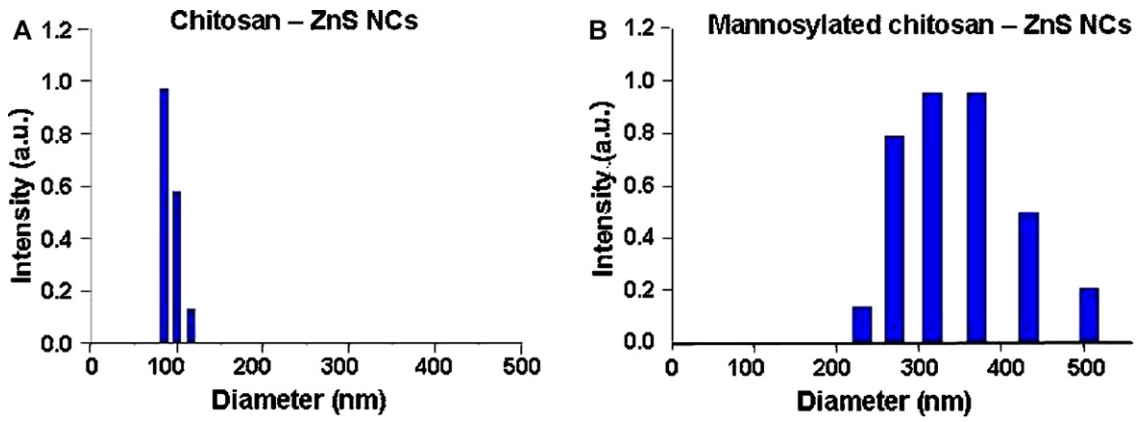

Fig. 3. Particle size distribution analysis using DLS of (A) chitosan-ZnS NCs and (B) mannosylated chitosan-ZnS NCs.

(Fig. 3B). The increase in particle size after bioconjugation with mannose can be due to the surface anchoring of mannose moieties to the amine groups present on the surface of chitosan-ZnS NCs.

This was further confirmed by the morphological analysis using scanning electron microscopy and atomic force microscopy respectively, as shown in Fig. 4. The SEM image of mannosylated chitosan-ZnS NCs clearly showed a homogeneous distribution of nearly monodisperse particles with spherical morphology, having size of ~150 nm. Particle size of the bioconjugated nanocrystals deduced from AFM also measured to be ~140 nm, which correlated well with the hydrodynamic diameter measured using DLS.

The infrared spectra of bare ZnS NCs showed a characteristic peak around 550 cm^{-1}, which is due to the Zn–S stretching vibrations. Chitosan displayed absorbances at 3421 cm^{-1} (O–H stretch overlapped with N–H stretch), 2923 and 2856 cm^{-1} (C–H stretch), 1650 cm^{-1} (amide I band, C=O stretch of acetyl group), 1309 (C–O stretching of primary alcoholic group), 1100 (–C–O–C–vibration) (Paulino, Simionato, Garcia, & Nozaki, 2006). For mannose sugar, aside of the broad O–H band in the 3400 cm^{-1} range, the minimum transmittance was in the 950–1200 cm^{-1} region where the C–O–C and C–O–H link band positions are found. The two shoulder peaks at 1145 and 1025 cm^{-1} can be attributed to the glycosidic links of mannose at α- (1 → 3) (Coimbra et al., 2005). The characteristic wave numbers that can be used for the quantification of mannose, *viz*., 1145, 1025 and 921 cm^{-1}, were present in mannosylated chitosan-ZnS NCs. FTIR studies on mannosylated chitosan-ZnS NCs displayed decreasing intensities with peak broadening for various bands of chitosan as well as of mannose, implying an interaction between these chemical moieties. This clearly confirmed the presence of chitosan and mannose in mannosylated chitosan-ZnS NCs.

Surface chemistry and thereby the surface capping ligands play a very critical role in determining the luminescence of nanocrystals by pacifying the dangling bonds at their surface. Fig. 5 represents the fluorescence emission from chitosan-ZnS NCs at various concentrations of chitosan, compared with that of bare ZnS nanocrystals. It is apparent that the fluorescence intensity decreases with increasing concentration of chitosan. The fluorescence intensity for the highest concentration of chitosan used (0.05 wt%), displayed a maximum of 38% quenching, with a slight blue shift in the peak emission wavelength from 610 to 595 nm. This can be attributed to the possible energy transfer that takes place from the molecular orbital levels of surface adsorbed chitosan to luminescent centers in doped ZnS, as observed in an earlier study on PVP capped ZnS (Manzoor, Vadera, Kumar, & Kutty, 2004). To achieve good surface passivation as well as luminescence intensity, we have optimized the concentration of chitosan at 0.01 wt%. At this concentration of chitosan used, it was noticed that the fluorescence emission in the visible wavelength range (~450 nm) attributed to the surface defect states in ZnS is clearly quenched, which indicates the appropriate surface passivation provided by chitosan chelation on ZnS. On mannosylation of chitosan-ZnS NCs (0.01 wt%), the fluorescence intensity was observed to decrease further, with a quenching of fluorescence up to ~40%. This result is contrary to the observations of 100% fluorescence quenching observed in CdSe or CdTe based quantum dots upon conjugation with proteins or dendrimers (Ghosh & Saha, 2009; Pan, Gao, He, Cui, & Zhang, 2006). This

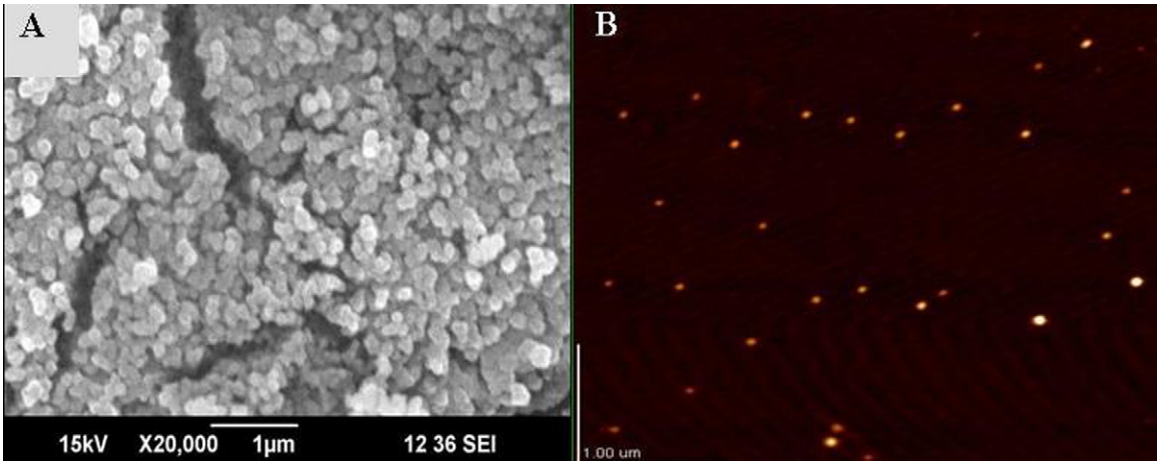

Fig. 4. Representative (A) SEM and (B) AFM images of mannosylated chitosan-ZnS NCs.

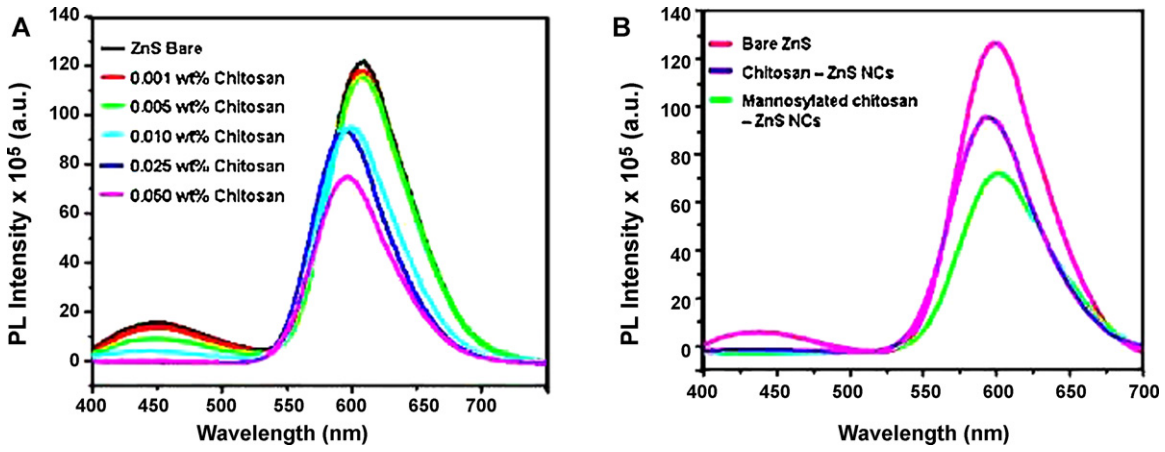

Fig. 5. Spectrofluorimetric analysis of (A) fluorescence emission intensity variations with different concentrations of chitosan and (B) fluorescence intensity variation for bare ZnS, 0.01 wt% chitosan-ZnS and mannosylated chitosan-ZnS NCs.

result stems from the fact that the fluorescence from Mn doped ZnS is size independent and arises from radiative transitions within the energy levels of dopant (Mn^{2+}) ions incorporated within the ZnS lattice. Our earlier studies on folic acid conjugated ZnS also reveal similar observations of fluorescence quenching at higher concentrations of folic acid (Manzoor et al., 2009). It is important to note that the visible luminescence at ~450 nm attributed to the surface defects in bare ZnS has been effectively passivated in chitosan-ZnS nanocrystals. The bright fluorescence emission from ZnS further to bioconjugation is an added advantage for targeted imaging or fluorescence based tracking, wherein long term florescence imaging of biological specimens becomes necessary.

3.2. Cytotoxicity studies

The toxicity effects of varying concentrations (0.1–100 μM) of bare and mannosylated chitosan-ZnS NCs on L929 and KB cell viability using MTT assay is given in Fig. 6. The results showed no signs of toxicity even up to higher doses of 100 μM and extended incubation periods of 48 h. This observation is in close comparison with our earlier reports of the non-toxic effects of ZnS upon conjugation with other biomolecules such as folic acid (Manzoor et al., 2009). It can be noticed from the interaction of mannosylated chitosan-ZnS NCs with mannose receptor over-expressing KB cells shown in Fig. 6B that the presence of the biopolymer chitosan and mannose sugar has helped to improve the cytocompatibility of the material.

3.3. Cancer imaging using mannosylated chitosan-ZnS NCs

Mannose functionalized chitosan-ZnS NCs emitting orange (~595 nm) colour were used at 10 μM concentration for imaging studies. The nanocrystals were incubated with the above cell lines in an appropriate culture medium for an hour before fixing for microscopy. Fig. 7 shows the bright field and fluorescent microscopy images of the specific targeting of mannosylated chitosan-ZnS NCs to oral cancer epithelial KB cells. A clear aggregation of a large concentration of the fluorescent nanocrystals can be evidently seen at the KB cell membrane in Fig. 7B and C. Interestingly, the cell morphology was not found to be altered upon interaction of the nanocrystals, suggesting their cytofriendly nature. The results of this *in vitro* targeted imaging of KB cells using carbohydrate conjugated nanocrystals essentially resemble the folate targeted nanocrystals studied earlier, wherein the cells individually as well as in colonies could be readily imaged using bioconjugated nanocrystals (Manzoor et al., 2009). Similarly, Kikkeri et al. (2009) have recently demonstrated an efficient *in vitro* and *in vivo* uptake of carbohydrate capped fluorescent QDs by liver cells by exploiting carbohydrate–protein interactions for specific targeting of tissues or organs *in vivo*.

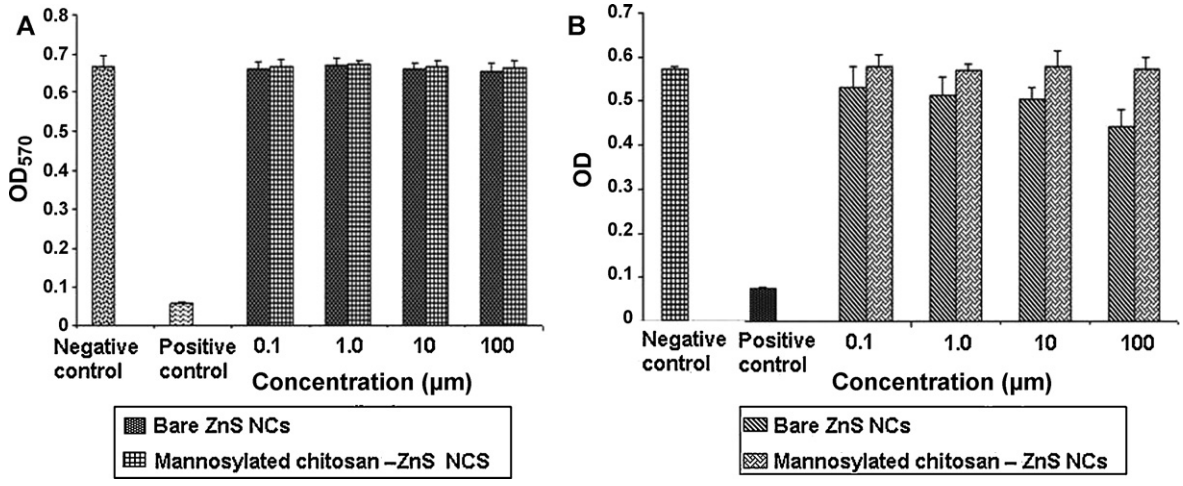

Fig. 6. Cytotoxicity analysis using MTT assay on (A) on normal mouse fibroblast cells (L929) and (B) oral cancer epithelial KB cells using bare ZnS and mannosylated chitosan-ZnS nanocrystals.

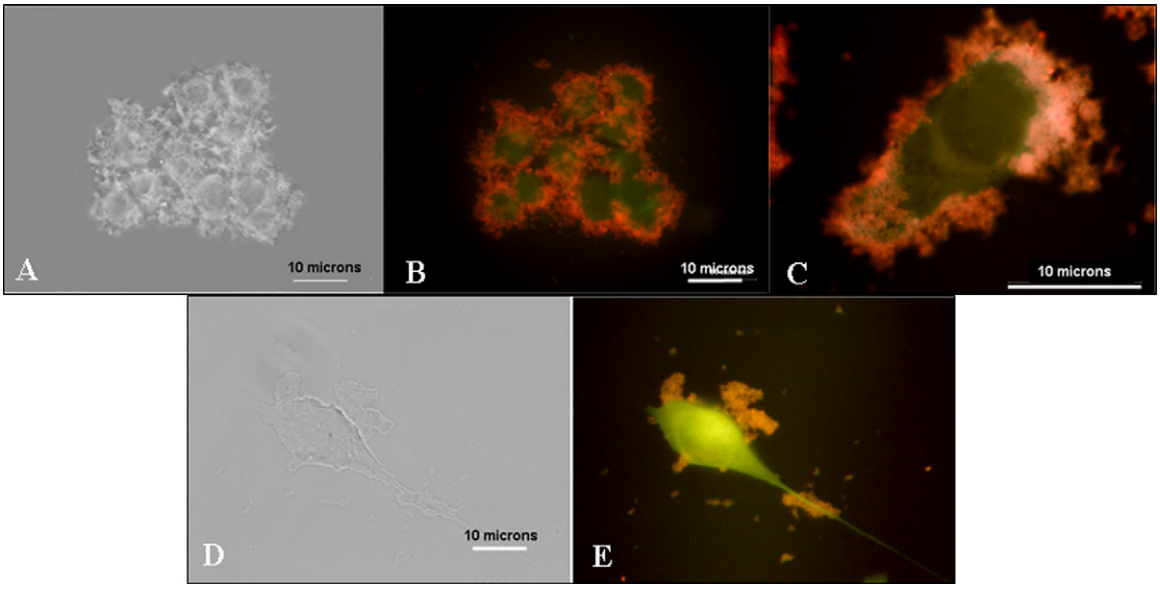

Fig. 7. Fluorescent microscopy images showing specific attachment of mannosylated chitosan-ZnS NCs to oral cancer epithelial KB cells (A) bright field and (B) fluorescent image of ZnS labelled KB cells at 40× magnification (C) 100× magnified image of a single KB cell labelled with mannosylated NCs (D) bright field and (E) fluorescent image of non-specific attachment of mannosylated NCs on normal fibroblast L929 cells at 40× magnification.

In contrast, the nature of this interaction changed dramatically upon use of the same concentration of nanocrystals on the normal mouse fibroblast L929 cells. As shown in Fig. 7D and E, due to absence of mannose receptors on the surface of the L929 cells, there was no specific attachment of the mannosylated chitosan-ZnS NCs onto these cells. The fluorescent nanocrystals were found randomly dispersed throughout the medium without any specific interaction with the cells. Hence, this served as control experiment wherein the nanocrystals showed minimum interaction with the normal cells.

One interesting feature as seen from the results above was the specific attachment of mannosylated chitosan-ZnS NCs to the outer membrane region of a colony of oral cancer epithelial cells. Such a distinct demarcation of cancer cells from a colony of cells will find immense use of these fluorescent nanocrystals for immunohistochemistry of tissue specimens. Further, the luminescence from the nanocrystals was bright and stable even after hours of continuous and repeated UV illumination, leading to the possibility of high-contrast imaging for extended durations. Our results thus clearly exemplify the feasibility of the use of the heavy metal-free, non-toxic, bioconjugated fluorescent ZnS nanocrystals for targeted cancer imaging. All these attributes of ZnS, added to its possibility of excitation using visible or near infrared radiation (using two-photon process enabled by its up-conversion characteristics) (Wei, Joly, Zhang, & Zhang, 2001) could render this doped nanocrystal useful also for targeted *in vivo* cancer imaging applications.

4. Conclusions

Aqueous suspension of mannosylated chitosan-ZnS NCs doped with Mn was prepared through a facile wet chemical route at room temperature. The natural biopolymer, chitosan, was used to provide multiple functions of stabilizing the nanocrystals against aggregation through steric hindrance, as well as providing appropriate functional groups for its bio-conjugation with a targeting ligand, *viz*., mannose. These water soluble, heavy metal-free, bioconjugated nanocrystals proved to be cytocompatible even at high doses (100 μM) and extended incubations (48 h). Interaction of the mannosylated nanocrystals with normal and cancer cells showed highly specific attachment of these fluorescent probes to mannose receptor over-expressing cancer cells, with minimal interference to normal cells. The bright and stable fluorescence of the nanocrystals enabled imaging of both single cancer cells as well as their colonies, without considerably altering their metabolic activity or morphology. Thus, we demonstrate the potential of fluorescent mannosylated chitosan-ZnS NCs for targeted cancer imaging applications.

Acknowledgements

DM would like to acknowledge the financial support from Department of Biotechnology, Government of India through the Rapid Young Investigator Grant No. BT/PR 8150/gbd/27/24/2006. AJ gratefully acknowledges University Grants Commission (UGC), Government of India, for her junior research fellowship. We gratefully acknowledge Dr. R. Jayakumar, Amrita Centre for Nanoscience and Molecular Medicine for his valuable suggestions in the manuscript preparation. The authors thank Mr. Girish C. M. and Mr. Sajin P. Ravi for SEM and AFM studies. The authors are also thankful for the support of Amrita Institute of Medical Sciences for infrastructure and lab maintenance support.

References

Agnani, G., Tricot-Doleux, S., Houalet, S., & Bonnaure-Mallet, M. (2003). Epithelial cell surface sites involved in the polyvalent adherence of *Porphyromonas gingivalis*: A convincing role for neuraminic acid and glucuronic acid. *Infection and Immunity*, *71*(2), 991–996.

Ashokan, A., Menon, D., Nair, S., & Manzoor, K. (2010). Molecular receptor targeted, hydroxyapatite nanocrystals based multi-modal contrast agent for magnetic resonance, X-ray and near-infrared fluorescence imaging. *Biomaterials*, *31*(9), 2606–2616.

Brevet, D., Gary-Bobo, M., Raehm, L., Richeter, S., Hocine, O., Amro, K., et al. (2009). Mannose-targeted mesoporous silica nanoparticles for photodynamic therapy. *Chemical Communications*, *28*(12), 1475–1477.

Bruchez, M., Moronne, M., Gin, P., Weiss, S., & Alivisatos, A. P. (1998). Semiconductor nanocrystals as fluorescent biological labels. *Science*, *281*, 2013–2016.

Chan, W. C. W., & Nie, S. M. (1998). Quantum dot bioconjugates for ultrasensitive nonisotopic detection. *Science*, *281*, 2016–2018.

Coimbra, M. A., Barros, A. S., Coelho, E., Gonçalves, F., Rocha, S. M., & Delgadillo, I. (2005). Quantification of polymeric mannose in wine extracts by FT-IR spectroscopy and OSC-PLS1 regression. *Carbohydrate Polymers*, *61*, 434–440.

Doty, R. C., Fernig, D. G., & Levy, R. (2004). Nanoscale science: A big step towards the Holy Grail of single molecule biochemistry and molecular biology. *Cellular and Molecular Life Sciences*, *61*, 1843–1849.

Gao, X., Cui, Y., Levenson, R. M., Chung, L. W. K., & Nie, S. (2004). *In vivo* cancer targeting and imaging with semiconductor quantum dots. *Nature Biotechnology*, *22*, 969–976.

Ghosh, S., & Saha, S. (2009). Synthesis and spectral properties of CdTe-dendrimer conjugates. *Nanoscale Research Letters*, *4*(8), 937–941.

Hezinger, A. F. E., Tessmar, J., & Goepferich, A. (2008). Polymer coating of quantum dots—A powerful tool toward diagnostics and sensorics. *European Journal of Pharmaceutics and Biopharmaceutics*, *68*, 138–152.

Jain, S. K., Gupta, Y., Jain, A., Saxena, A. R., Khare, P., & Jain, A. (2008). Mannosylated gelatin nanoparticles bearing an anti-HIV drug didanosine for site-specific delivery. *Nanomedicine: Nanotechnology, Biology and Medicine*, *4*, 41–48.

Jayakumar, R., Menon, D., Manzoor, K., Nair, S. V., & Tamura, H. (2010). Biomedical applications of chitin and chitosan based nanomaterials—A short review. *Carbohydrate Polymers*, *82*(2), 227–232.

Kang, M. L., Cho, C. S., & Yoo, H. S. (2009). Application of chitosan microspheres for nasal delivery of vaccines. *Biotechnology Advances*, *27*, 857–865.

Kikkeri, R., Lepenies, B., & Adibekian, A. (2009). *In vitro* imaging and *in vivo* liver targeting with carbohydrate capped quantum dots. *Journal of American Chemical Society*, *131*, 2110–2112.

Kumar, M. N. V. R., Muzzarelli, R. A. A., Muzzarelli, C., Sashiwa, H., & Domb, A. J. (2004). Chitosan chemistry and pharmaceutical perspectives. *Chemical Reviews*, *104*(12), 6017–6084.

Lane, K. B., Egan, B., Vick, S., Abdolrasulnia, R., & Shepherd, V. L. (1998). Characterization of a rat alveolar macrophage cell line that expresses a functional mannose receptor. *Journal of Leukocyte Biology*, *64*, 345–350.

Lee, J. H., Kim, Y. A., Kim, K., Huh, Y. D., Hyun, J. W., Kim, H. S., et al. (2007). Synthesis and optical properties of the water-dispersible ZnS:Mn nanocrystals surface capped by L-aminoacid ligands: Arginine, cysteine, histidine, and methionine. *Bulletin of the Korean Chemical Society*, *28*(7), 1091–1096.

Li, Y, Chen, J., Zhu, C., Wang, L., Zhao, D., Zhuo, S., et al. (2004). Preparation and application of cysteine capped ZnS nanoparticles as fluorescence probe in the determination of nucleic acids. *Spectrochemica Acta Part A*, *60*, 1719–1724.

Lovric, J., Sung, J. C., & Francoise, M. W. (2005). Unmodified Cadmium Telluride quantum dots induce reactive oxygen species formation leading to multiple organelle damage and cell death. *Chemistry & Biology*, *12*(11), 1227–1234.

Manzoor, K., Johny, S., Thomas, D., Setua, S., Menon, D., & Nair, S. (2009). Bioconjugated luminescent quantum dots of doped ZnS: A cyto-friendly system for targeted cancer imaging. *Nanotechnology*, *20*, 065102–065115.

Manzoor, K., Vadera, S. R., Kumar, N., & Kutty, T. R. N. (2003). Synthesis and photoluminescent properties of ZnS nanocrystals doped with copper and halogen. *Materials Chemistry and Physics*, *82*, 718–725.

Manzoor, K., Vadera, S. R., Kumar, N., & Kutty, T. R. N. (2004). Energy transfer from organic surface adsorbate-polyvinyl pyrrolidone molecules to luminescent centers in ZnS nanocrystals. *Solid State Communications*, *129*, 469–473.

Mathew, M. E., Mohan, J. C., Manzoor, K., Nair, S. V., Tamura, H., & Jayakumar, R. (2010). Folate conjugated carboxymethyl chitosan–manganese doped zinc sulphide nanoparticles for targeted drug delivery and imaging of cancer cells. *Carbohydrate Polymers*, *80*, 443–449.

Mattoussi, H., Mauro, J. M., Goldman, E. R., Green, T. M., Anderson, G. P., Sundar, V. C., et al. (2001). Bioconjugation of highly luminescent colloidal CdSe–ZnS quantum dots with an engineered two domain recombinant protein. *Physica Status Solidi B-Basic Research*, *224*, 277–283.

Medintz, I. L., Uyeda, H. T., Goldman, E. R., & Mattoussi, H. (2005). Quantum dot bioconjugates for imaging, labelling and sensing. *Nature Materials*, *4*, 435–446.

Mitchell, J. P., Roberts, D. R., Langley, J., Koentgen, F., & Lambert, J. N. (1998). A direct method for the formation of peptide and carbohydrate dendrimers. *Bioorganic and Medicinal Chemistry Letters*, *9*, 2785–2788.

Muzarelli, R. A. A. (2011). Potential of chitin/chitosan-bearing materials for uranium recovery:An interdisciplinary review. *Carbohydrate Polymers*, *81*(1), 54–63.

Nie, Q., Tan, W. B., & Zhang, Y. (2006). Synthesis and characterization of monodisperse chitosan nanoparticles with embedded quantum dots. *Nanotechnology*, *17*(1), 0–144.

Pan, B., Gao, F., He, R., Cui, D., & Zhang, Y. (2006). Study on interaction between poly (amidoamine) dendrimer and CdSe nanocrystal in chloroform. *Journal of Colloid and Interface Science*, *297*, 151–156.

Paulino, A. T., Simionato, J. I., Garcia, J. C., & Nozaki, J. (2006). Characterization of chitosan and chitin produced from silkworm crysalides. *Carbohydrate Polymers*, *64*, 98–103.

Pradhan, N., David, M. B., Liu, Y., & Peng, X. (2007). Efficient, stable, small and water-soluble doped ZnSe nanocrystal emitters as non-cadmium biomedical labels. *Nano Letters*, *7*(2), 312–317.

Raiber, E., Tulone, C., Zhang, Y., Martinez-Pomares, L., Steed, E., Sponaas, A. M., et al. (2010). Targeted delivery of antigen processing inhibitors to antigen presenting cells *via* mannose receptors. *ACS Chemical Biology*, *5*(5), 461–476.

Setua, S., Menon, D., Asok, A., Nair, S., & Manzoor, K. (2010). Folate receptor targeted, rare-earth oxide nanocrystals for bi-modal fluorescence and magnetic imaging of cancer cells. *Biomaterials*, *31*(4), 714–729.

Smith, A. M., Duan, H., Mohs, A. M., & Nie, S. (2008). Bioconjugated quantum dots for *in vivo* molecular and cellular imaging. *Advanced Drug Delivery Reviews*, *60*(11), 1226–1240.

Steele, C., Leigh, J., Swoboda, R., Ozenci, H., & Fidel, P. L. (2001). Potential role for a carbohydrate moiety in anti-*candida* activity of human oral epithelial cells. *Infection and Immunity*, *69*(11), 7091–7099.

Warad, H. C., Thanachayanont, C., Tumcharern, G., & Dutta, J. (2007). Chitosan clad manganese doped zinc sulphide nanoparticles as biological labels. In *Nano/Micro Engineered and Molecular Systems, 2007. NEMS '07. 2nd IEEE International Conference* Bangkok, (pp. 342–346).

Wei, C., Joly, A. G., Zhang, & Zhang, J. Z. (2001). Up-conversion luminescence of Mn^{2+} in ZnS:Mn^{2+} nanoparticles. *Physical Review B*, *64*, 041202–041206.

Xie, M., Liu, H., Chen, P., Zhang, Z., Wang, X., Xie, Z., et al. (2005). CdSe/ZnS-labeled carboxymethyl chitosan as a bioprobe for live cell Imaging. *Chemical Communications*, *44*, 5518–5520.

Yang, H., Santra, S., & Holloway, P. H. (2005). Synthesis and applications of Mn-doped II–VI semiconductor nanocrystals. *Journal of Nanoscience and Nanotechnology*, *5*, 1364–1375.

Yu, W. W., Chang, E., Drezek, R., & Colvin, V. L. (2006). Water-soluble quantum dots for biomedical applications. *Biochemical and Biophysical Research Communications*, *348*, 781–786.

Zhuang, J., Zhang, X., Wang, G., Li, D., Yang, W., & Li, T. (2003). Synthesis of water-soluble ZnS:Mn^{2+} nanocrystals by using mercaptopropionic acid as stabilizer. *Journal of Materials Chemistry*, *13*, 1853–1857.